Universiteit Utrecht

Simulating sessile fluid droplets in fluid-fluid interfaces or on deformable solid surfaces

June 18, 2014

Author:
Robin van Damme

Supervisors:
Rene van Roij
Giuseppe Soligno

Abstract

In this thesis we describe a method of numerically computing the shape of a two-dimensional droplet of fluid, either suspended in a fluid-fluid interface or resting upon a deformable solid surface. This is done by minimizing the relevant free energies of the system, taking into account surface energy, gravitational energy and elastic energy. Given are expressions for the separate contributions to this free energy and their discretized counterparts. A brief description of the algorithm used is also given.

Contents

1 An introduction to the subject

The system we will be studying is that of a droplet of liquid either suspended in a fluid-fluid interface or resting upon the surface of a solid. Assuming that the fluid-fluid interface or the solid surface is flat (or that the droplet is small enough to approximate it as such), it is possible to describe a two-dimensional slice of this droplet by two functions describing the height $H(x)$ and depth $h(x)$ of respectively the liquid-vapor and the solid-liquid interface. The two-dimensional system we study in this thesis is a y-symmetric slab of droplet. In other words, it is not a rotationally symmetric slice of a three-dimensional droplet. However, generalizing to a representation of a three-dimensional system is straightforward. See figure 1 for an illustration.

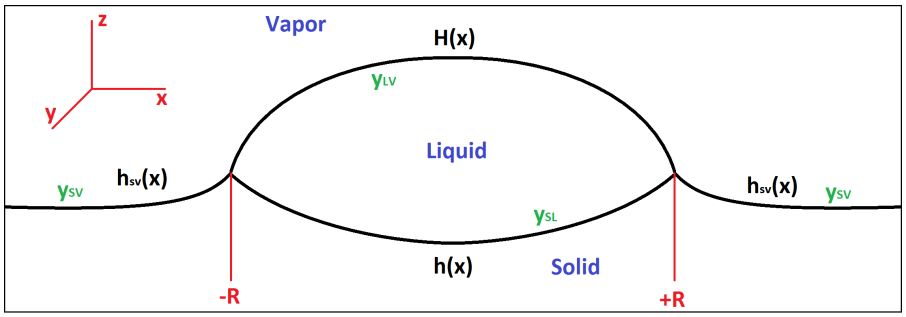

Figure 1: This image shows the system we are studying and how it is parametrized. A droplet of liquid rests upon a solid surface, with a vapor (generally, any fluid) above it. The system is described by the surface free energies, the functions $H(x)$, $h(x)$ and the droplet width $2R$. We will not study the deformation of the solid described by h_{SV} here, as it is usually negligibly small [1].

2 Goals of this thesis

This research was started with a paper by Lubbers [1], who introduced an expression for the elastic free energy for a two-dimensional droplet slice in terms of a (double) Fourier transform over a function $h(x)$ describing the depth of the liquid-solid interface at a certain position x. Combined with the method used by Soligno [6], I believed it was possible to calculate the full shape of a two-dimensional slab of droplet on a deformable solid surface and observe the influence of elasticity on this shape. I believe I have succeeded in doing so, and this thesis should serve to explain all steps necessary for replicating my research and algorithm.

3 Theory of contact angles

3.1 Contact angles: Young and Neumann

Even a system as seemingly mundane as a droplet lying on a surface can display some interesting physical phenomena. The phenomenon of droplet formation on surfaces is known as wetting, and can be studied in terms of so-called contact angles. The inclusion of elasticity and the transition between macroscopic and microscopic descriptions of contact angles is still an active area of research [1] [4] [5] [8]. Contact angles define the slopes of the various interfaces of the three-phase contact line of the system, and uniquely define equilibrium solutions of droplet shapes. Any equilibrium configuration must satisfy a force balance on the three-phase contact line. Although there are some subtleties (most notably being the Shuttleworth effect, as explained later, see also [5]), this force balance can for three dimensions be derived from simple geometry and written as follows:

$$\gamma_{\alpha\theta} + \gamma_{\theta\beta}\cos\theta + \gamma_{\alpha\beta}\cos\alpha = 0 \tag{1}$$

$$\gamma_{\alpha\theta}\cos\theta + \gamma_{\theta\beta} + \gamma_{\alpha\beta}\cos\beta = 0 \tag{2}$$

$$\gamma_{\alpha\theta}\cos\alpha + \gamma_{\theta\beta}\cos\beta + \gamma_{\alpha\beta} = 0 \tag{3}$$

The angles α, β and θ are as in figure 2, and the free energies per unit surface γ_{AB} are those corresponding to the phases the angles describe. For the specific case where we look at a two-dimensional

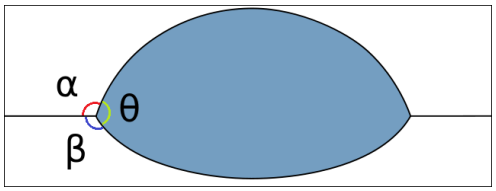

Figure 2: A droplet on a deformed solid surface. The shape is characterized by three contact angles α, β and θ. These angles depend on the free energies per unit surface of the interfaces.

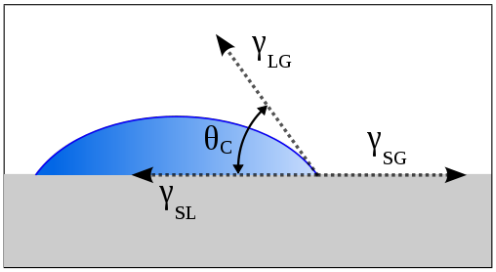

Figure 3: A simple case of wetting. The contact angle θ_C describes a ratio between the surface free energies γ_{SL}, γ_{LG} and γ_{SG}, following Young's law.

x-z slice of this droplet and we have a perfectly rigid flat surface, equation 2 generalizes to what is known as Young's law. This is done by taking $\beta = \pi$, and filling in the relevant phases for the γ_{ab}'s. For example, filling in the phases corresponding to figure 3 would give us:

$$\gamma_{SG} - \gamma_{SL} = \gamma_{LG} \cos\theta$$

A simulation for determining the shape of a droplet following Young's law has been done by Giuseppe Soligno, whose work served as a basis for the presently described work. It should also be noted that the formulation of a force balance as in equations 1, 2, and 3 implies that none of the three surface free energies may be greater than the sum of the other two if an equilibrium solution is to exist. We will use this later on to decide what parameter values to choose for the γ's in our simulation.

3.2 Shuttleworth effect

For systems that are compressible, the surface stress[1]along an interface is not necessarily equal to the surface free energy of this interface. The relation between these two quantities is given by the Shuttleworth equation [9]:

$$\Upsilon = \gamma + \frac{d\gamma}{d\epsilon_{\parallel}} \quad ,$$

where Υ is the surface stress, γ is the interfacial surface free energy and $\epsilon_{\parallel}$ is the elastic strain[2](deformation) parallel to the surface. Essentially this equation tells us that if one of the phases involved is compressible, then $\Upsilon \neq \gamma$ and we cannot set up the force balances as in section . The elastic free energy is also influenced by compressibility, and the Shuttleworth effect is directly responsible for any tangential elastic displacements around a contact line [1][7]. In this thesis we will consider the case where the Shuttleworth effect is absent; i.e. there are no tangential displacements and we can safely assume that $\Upsilon = \gamma$.

4 Theory of free energies

In thermodynamics, systems at fixed temperature will generally change to a configuration that minimizes the free energy. To find equilibrium configurations is therefore the same as finding the minimum free energy state. Usually, though, the type of systems studied are comprised of many particles, and have many degrees of freedom. Finding minima can be a challenge, but is sometimes possible if the system is cleverly parametrized.

For our system we will consider three contributions to the free energy:

- The surface free energy $\mathcal{F}_s$, describing the energy cost involved in creating a surface.
- The gravitational energy $\mathcal{F}_g$.
- The elastic energy $\mathcal{F}_E$, which is the energy cost of elastic deformation of the solid that the droplet rests upon.

4.1 Surface energy

The free energy of the interfaces can be expressed by the total surface area of this interface times a parameter γ which is the amount of energy per unit surface. For our two-dimensional system, the surface area of the interface is given by the arc length of the line describing it. In other words: it is given by the arc length of the function $h(x)$ or $H(x)$. In the case of our droplet, the arc length is given by the integral:

$$A_{LV} = \int_{-R}^{+R} \left(1 + H'(x)^2\right)^{1/2} dx$$

For the lower interface it is just so:

$$A_{SL} = \int_{-R}^{+R} \left(1 + h'(x)^2\right)^{1/2} dx$$

For the vapor/solid interface we can express the SV interface area as the total surface area A_{tot} of the solid-vapor interface (which is a constant) minus the SV interfacial area 'missing' due to the presence of the droplet.

[2]The surface stress is a quantity with units force per unit length that expresses the amount of force acting on a unit of surface of an interface.

[2]The elastic strain is nothing more than the deformation of the solid surface along the axis parallel to the flat undeformed solid surface.

Under the assumption that the solid-vapor interface is always flat, this area is simply the width of the droplet, $2R$. So we have:

$$A_{SV} = A_{tot} - 2R$$

The surface free energy is then given by these areas multiplied by their respective γ's.

$$\begin{aligned}\mathcal{F}_s &= \gamma_{LV} A_{LV} + \gamma_{SL} A_{SL} + \gamma_{SV} A_{SV} \\ &= \gamma_{LV} \int_{-R}^{+R} \left(1 + H'(x)^2\right)^{1/2} dx + \gamma_{SL} \int_{-R}^{+R} \left(1 + h'(x)^2\right)^{1/2} dx + \gamma_{SV}(A_{tot} - 2R)\end{aligned}$$

Given that we are only interested in minimizing this free energy, we can subtract the constant $\gamma_{SV} A_{tot}$ from the total energy and call this the new energy we want to minimize. So the final surface terms become:

$$\mathcal{F}_s = \gamma_{LV} \int_{-R}^{+R} \left(1 + H'(x)^2\right)^{1/2} dx + \gamma_{SL} \int_{-R}^{+R} \left(1 + h'(x)^2\right)^{1/2} dx - 2\gamma_{SV} R$$

4.2 Gravitational energy

We also include the effect of gravity in our simulation. Given that $H(x)$ describes the height of the liquid-vapor interface and $h(x)$ the depth of the liquid-solid interface, an infinitesimal volume slice of the liquid is given by $(H(x) + h(x))\, dx$. Of course, the volume occupied by the liquid must have displaced part of the solid and/or vapor, so the gravitational energy will depend on their respective differences in density:

$$\mathcal{F}_g = g \int_{-R}^{+R} \left((\rho_L - \rho_V) \int_0^{H(x)} z dz + (\rho_S - \rho_L) \int_{h(x)}^{0} z dz \right) dx = \frac{1}{2} g \int_{-R}^{+R} \left(\Delta\rho_{LV} H(x)^2 - \Delta\rho_{SL} h(x)^2 \right) dx \quad ,$$

where we rewrite all constants to an absolute energy scale $G = \frac{1}{2} g \Delta\rho_{LV}$ and a relative energy scale $\Delta_\rho = \frac{\Delta\rho_{SL}}{\Delta\rho_{LV}} = \frac{\rho_S - \rho_L}{\rho_L - \rho_V}$. Note that generally $\rho_L > \rho_V$, but not necessarily $\rho_S > \rho_L$. If the liquid is denser than the solid, there will be a net force pushing the liquid up.

$$\mathcal{F}_g = \frac{1}{2} g \Delta\rho_{LV} \int_{-R}^{+R} \left(H(x)^2 - \frac{\Delta\rho_{SL}}{\Delta\rho_{LV}} h(x)^2 \right) dx = G \int_{-R}^{+R} \left(H(x)^2 - \Delta_\rho h(x)^2 \right) dx$$

4.3 Elastic energy

The main area of research of this thesis is the effect of the elastic energy. While the gravitational and surface energies are fairly trivial to derive, the elastic energy is not. The expression used in this thesis will be one that was derived by Frederickson *et al.* [3] for the case of a solid consisting of long polymer chains, and later generalized by Long *et al.* [2] for any solid. In Frederickson's paper the authors derive an expression for the elastic energy for a deformation of a solid surface described by the function $h(x) = h_0 + \epsilon \cos qx$ under the assumption that $\epsilon \ll h_0$. In the same paper they also generalize this to the following expression for a deformation given by $z = h(x, y)$:

$$\mathcal{F}_E = \frac{1}{2} \int \frac{d^2 q}{(2\pi)^2} P(\mathbf{q}) h(\mathbf{q}) h(-\mathbf{q}) \quad ,$$

where $h(\mathbf{q})$ describes the two-dimensional Fourier transform of $h(x, y) - h_0$ and $P^{-1}(q)$ a susceptibility related to the pair correlation function of height fluctuations at the surface of the brush (*deformation*)[3]. Frederickson's full derivation for this result is beyond the scope of this thesis. Instead, we will use the expression provided by Long:

$$\mathcal{F}_E = \frac{E}{2} \int_{-\infty}^{\infty} \frac{dq}{2\pi} \hat{Q}(q) \left[\hat{h}(q) \hat{h}(-q) + \hat{u}(q) \hat{u}(-q) \right]$$

Here, $\hat{h}(q)$ are again the Fourier transform of $h(x)$, but $h(x)$ only describes normal displacements at the surface. The terms $\hat{u}(q)$ are the Fourier transform of the function $u(x)$ describing the tangential displacements, which disappear if the solid is incompressible [7][4][5]. Furthermore we have $\hat{Q}(q)$, which is a Green's function that in the incompressible limit reads $\hat{Q}(q) = 2|q|/3$ and E being the elastic modulus of the solid. Rewriting a little bit:

$$\mathcal{F}_E = \frac{E}{4\pi} \int_{-\infty}^{\infty} \frac{2|q|}{3} \hat{h}(q) \hat{h}(-q) dq$$

5 Numerics

5.1 Rough outline

Minimization (or rather, optimization) problems are a thoroughly studied area in computational sciences and in statistical physics. Especially often-used in statistical physics are Monte Carlo simulations. In this thesis we will use a particular type of Monte-Carlo simulation known as the Metropolis-Hastings algorithm, and drive the system to a minimum by means of so-called simulated annealing. The method of simulated annealing is obtained by taking the Metropolis algorithm, making the acceptance criterion P depend on temperature and energy difference, and adding a gradually lowering temperature. Figure 5 describes at a very basic level what our algorithm does, and how it uses the aforementioned methods.

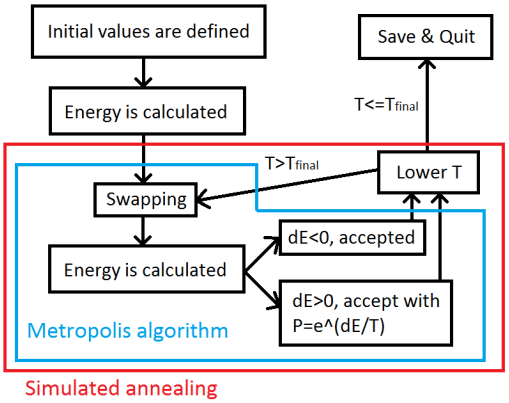

Figure 4: The algorithm in short.

To describe the droplet shape, we discretize the functions $H(x)$ and $h(x)$ by describing them by an array describing rectangles of fixed width and variable height. We also define a separate number that will define the width of the droplet, the base. There are two reasons for doing this:

- Both $H(x)$ and $h(x)$ must go to zero at $\pm R$. In other words, the boundaries of both functions must be the same. While it is possible to get the width of the droplet from looking at the amount of nonzero height array elements, this could violate our condition that both functions have the same boundaries.
- Because the width is used as a separate parameter in the surface free energy, it needs to have a high spatial resolution to accurately find minimum energy configurations. If the width was determined by the amount of nonzero height elements (which is an integer value), the amount of elements would have to be very large to allow for the same resolution as taking a real[3] value to represent the width.

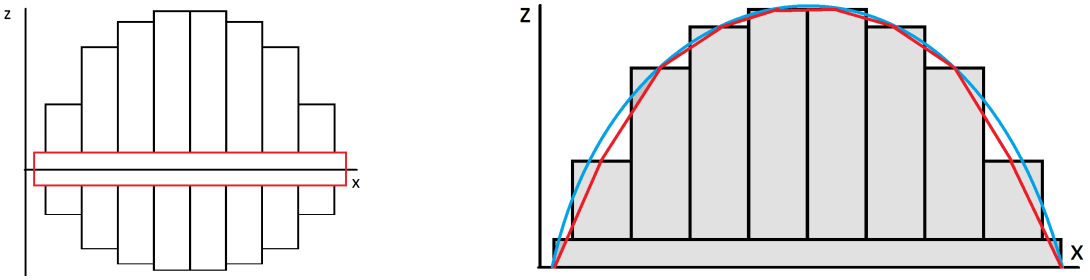

Figure 5: Left: a visual representation of our numerical description of the functions $H(x)$ (up), $h(x)$ (down) and the base (in red). Right: In red the surface as calculated, in blue the analytical droplet shape that we're trying to find.

We now have the discrete versions $H(x) \to \Delta_x H_x$, $h(x) \to \Delta_x h_x$, $2R \to \Delta_x B$, where $x = \Delta_x n$ with n an integer value and Δ_x a constant with the dimensions of distance. The values H_x, h_x and B are now pure numbers.

5.2 Metropolis algorithm / Simulated annealing

To minimize the free energy, we use the method of simulated annealing, a modified Metropolis-Hastings algorithm. The Metropolis-Hastings algorithm is a rather general algorithm that can be used to find extrema. Starting from an initial value y, one randomly samples a value y' based on a probability distribution, and selects whether to accept or reject this candidate based on a criterion $P(y, y')$. If it is accepted, $y \to y'$, and if it is rejected $y \to y$.

To tailor this algorithm to our minimization criteria, we take the following steps:

- Let the value y be given by the free energy corresponding to the current droplet shape.
- Let y' be given by the new droplet shape after we have randomly swapped two volume elements. The available swaps are defined in the next paragraph.

[3]Real value as represented numerically by a double precision floating point value.

- The acceptance criterion $P(y, y')$ is given by the difference in free energy between the states y and y': $\Delta\mathcal{F} = \mathcal{F}_{y'} - \mathcal{F}_y$. If $\Delta\mathcal{F} < 0$, the new shape is accepted, and if $\Delta\mathcal{F} > 0$, the shape is accepted only with a probability $P = e^{\Delta\mathcal{F}/T}$, where T is a parameter that describes the "temperature" of the system.[4]This parameter effectively describes the size of the energy fluctuations that are allowed tol occur in the minimization process.
- After a set amount of Metropolis cycles M of repeating the above three steps, we lower T so that the net size of energy fluctuations goes down. This leads to what is known as simulated annealing, where a thermodynamic system cooling down is simulated.

5.3 Swaps

In order to vary the shape of the droplet, we need to be able to vary the functions $H(x)$ and $h(x)$ and the width of the droplet $2R$. To do this, we fix the total volume of the droplet by defining an initial configuration with volume V, and only allow H_x, h_x and B to vary by swapping volume in between them. We define four possible ways to swap volume during one Metropolis cycle:

1. **Horizontal swaps on the upper part of the droplet:**
   Volume is swapped from an element of the array H_x to a neighbouring element in the array.
   - 1.1 A random amount of volume ΔV in the range $[0, \Delta V_{max}]$ is defined to be swapped.
   - 1.2 An element k is randomly chosen out of all nonzero elements in the H_x array.
   - 1.3 A random number of value $+1$ or -1 is generated, each with 50% probability. This number is added to k. This step is required to fulfill the detailed balance principle.
   - 1.4 A random number $\bar{k}$ of value $+1$ or -1 is generated, each with 50% probability.
   - 1.5 Volume ΔV is subtracted from H_k and added to $H_{k+\bar{k}}$. If $H_k - dV < 1.0$, all volume in H_k is swapped. This minimum value can be chosen freely, but is in our case set to 1.0 to prevent instability of the simulation.
2. **Horizontal swaps on the lower part of the droplet:**
   Volume is swapped from an element of the array h_x to a neighbouring element in the array.
   - 2.1 A random amount of volume ΔV in the range $[0, \Delta V_{max}]$ is defined to be swapped.
   - 2.2 An element k is randomly chosen out of all nonzero elements in the h_x array.
   - 2.3 A random number of value $+1$ or -1 is generated, each with 50% probability. This number is added to k. This step is required to fulfill the detailed balance principle.
   - 2.4 A random number $\bar{k}$ of value $+1$ or -1 is generated, each with 50% probability.
   - 2.5 Volume ΔV is subtracted from h_k and added to $h_{k+\bar{k}}$. If $h_k - dV < 1.0$, all volume from h_k is swapped. This minimum value can be chosen freely, but is in our case set to 1.0 to prevent instability of the simulation.
3. **Internal swaps between the base and the upper part of the droplet:**
   Volume is swapped between the base B and the upper array H_x.
   - 3.1 A random amount of volume ΔV in the range $[0, \Delta V_{max}]$ is defined to be swapped.
   - 3.2 A random number r of value $+1$ or -1 is generated.
   - 3.3 An element k is randomly chosen out of all nonzero elements in the H_x array.
   - 3.4 If $r = +1$, volume ΔV is subtracted from H_k and added to B. If $H_k - \Delta V < 1.0$, all volume from H_k is swapped.
   - 3.5 If $r = -1$, volume ΔV is subtracted from B and added to H_k. If $B - \Delta V < 1.0$, all volume from B is swapped.
4. **Internal swaps between the base and the lower part of the droplet:**
   Volume is swapped between the base B and the lower array h_x.
   - 4.1 A random amount of volume ΔV in the range $[0, \Delta V_{max}]$ is defined to be swapped.

[4]Physically, to get the right dimensions this parameter T should of course be $k_B T$, where k_B is the Boltzmann constant and T the actual temperature. For our simulation, however, we will rescale the free energy to a dimensionless number. T will then also simply be a number.

4.2 A random number r of value $+1$ or -1 is generated.

4.3 An element k is randomly chosen out of all nonzero elements in the h_x array.

4.4 If $r = +1$, volume ΔV is subtracted from h_k and added to B. If $h_k - \Delta V < 1.0$, all volume from h_k is swapped.

4.5 If $r = -1$, volume ΔV is subtracted from B and added to h_k. If $B - \Delta V < 1.0$, all volume from B is swapped.

5.4 Discretized free energies

We now need to discretize our free energies in terms of our numerical approximation.

5.4.1 Surface energy

We start off with the expression found in 4.1:

$$\mathcal{F}_s = \gamma_{LV} \int_{-R}^{+R} \left(1 + H'(x)^2\right)^{1/2} dx + \gamma_{SL} \int_{-R}^{+R} \left(1 + h'(x)^2\right)^{1/2} dx - 2\gamma_{SV} R$$

From here, we discretize the arc lengths to a sum over distances between the centers of the rectangles of height H_x or depth h_x:

$$\int_{-R}^{+R} \left(1 + H'(x)^2\right)^{1/2} dx \to \sum_x \left(\Delta_x^2 + (H_{x+1} - H_x)^2\right)^{1/2}$$

$$\int_{-R}^{+R} \left(1 + h'(x)^2\right)^{1/2} dx \to \sum_x \left(\Delta_x^2 + (h_{x+1} - h_x)^2\right)^{1/2}$$

The liquid-vapor and solid-liquid interfaces are only defined from $-R$ to $+R$. Numerically, they are only defined where there is volume. In other words, only for nonzero array elements. We therefore introduce four new parameters: U_L, U_R, D_L, D_R. These represent the index of the leftmost and rightmost nonzero array elements, which are the elements where the droplet starts and ends, if summing from 0 upwards. Filling in these boundaries in the sums, we get:

$$\sum_{x=U_L}^{U_R-1} \left(\Delta_x^2 + \Delta_x^2 (H_{x+1} - H_x)^2\right)^{1/2} = \Delta_x \sum_{x=U_L}^{U_R-1} \left(1 + (H_{x+1} - H_x)^2\right)^{1/2}$$

$$\sum_{x=D_L}^{D_R-1} \left(\Delta_x^2 + \Delta_x^2 (h_{x+1} - h_x)^2\right)^{1/2} = \Delta_x \sum_{x=D_L}^{D_R-1} \left(1 + (h_{x+1} - h_x)^2\right)^{1/2}$$

The only thing we now need to include is the surface we gain from connecting the edges of the upper and lower part of the droplet to the base B. Under the assumption that the equilibrium droplet shape is symmetric about its x-center, we can state that the horizontal separation between the base and the first nonzero element and the base and the last nonzero element are the same. This allows us to determine the horizontal distance by simply taking the difference in width between the respective array and the value of the base B. Because the base is at $z = 0$, the vertical distance is simply given by the mean height of the edges of the height array plus half the slab height Δ_x. The extra surface is then given by:

$$2\Delta_x \left(\left(\frac{U_R - U_L}{2} - \frac{B}{2} \right)^2 + \left(\frac{H_{U_L} + H_{U_R} + 1}{2} \right)^2 \right)^{1/2} = \Delta_x \left((U_R - U_L - B)^2 + (H_{U_L} + H_{U_D} + 1)^2 \right)^{1/2}$$

And likewise for the lower array:

$$2\Delta_x \left(\left(\frac{D_R - D_L}{2} - \frac{B}{2} \right)^2 + \left(\frac{h_{D_L} + h_{D_R} + 1}{2} \right)^2 \right)^{1/2} = \Delta_x \left((D_R - D_L - B)^2 + (h_{D_L} + h_{D_R} + 1)^2 \right)^{1/2}$$

The total expression for the discretized free surface energy then becomes:

$$\mathcal{F}_s = \gamma_{LV} \Delta_x \left(\left(\sum_{x=U_L}^{U_R-1} \sqrt{1 + (H_{x+1} - H_x)^2} \right) + \sqrt{(U_R - U_L - B)^2 + (H_{U_L} + H_{U_R} + 1)^2} \right)$$

$$+\gamma_{SL}\Delta_x\left(\left(\sum_{x=D_L}^{D_R-1}\sqrt{1+(h_{x+1}-h_x)^2}\right)+\sqrt{(D_R-D_L-B)^2+(h_{D_L}+h_{D_R}+1)^2}\right)-\gamma_{SV}\Delta_x B \quad ,$$

which we rewrite to one absolute and two relative energy scales to obtain the final expression:

$$\mathcal{F}_s=\gamma_{LV}\Delta_x\Bigg[\left(\left(\sum_{x=U_L}^{U_R-1}\sqrt{1+(H_{x+1}-H_x)^2}\right)+\sqrt{(U_R-U_L-B)^2+(H_{U_L}+H_{U_R}+1)^2}\right)$$

$$+\frac{\gamma_{SL}}{\gamma_{LV}}\left(\left(\sum_{x=D_L}^{D_R-1}\sqrt{1+(h_{x+1}-h_x)^2}\right)+\sqrt{(D_R-D_L-B)^2+(h_{D_L}+h_{D_R}+1)^2}\right)-\frac{\gamma_{SV}}{\gamma_{LV}}B\Bigg]$$

We will use $\gamma_{LV}\Delta_x$ to scale our system. We divide all energy contributions by $\gamma_{LV}\Delta_x$ to make them dimensionless.

$$\mathcal{F}=\mathcal{F}_s+\mathcal{F}_g+\mathcal{F}_E\rightarrow f=\mathcal{F}/\gamma_{LV}\Delta_x=f_S+f_G+f_E$$

5.4.2 Gravitational energy

Starting from the expression in 4.2:

$$\mathcal{F}_g=g\Delta\rho_{LV}\int_{-R}^{+R}\left(H(x)^2-\frac{\Delta\rho_{SL}}{\Delta\rho_{LV}}h(x)^2\right)dx=G\int_{-R}^{+R}\left(H(x)^2-\Delta_\rho h(x)^2\right)dx$$

we can use G and Δ_ρ as absolute and relative energy scales. The rest of the discretization is straightforward:

$$\mathcal{F}_g=\Delta_x G\left(\sum_{x=U_L}^{U_R}H_x^2-\Delta_\rho\sum_{x=D_L}^{D_R}h_x^2\right)$$

The base, representing a z-symmetric slab on the chosen $z=0$ axis, also contributes to the gravitational energy if $\Delta_\rho\neq 1$. Splitting the slab in two to calculate the separate contributions gives us the upper slab with volume $\frac{1}{2}\Delta_x B$ and gravitational energy $+\frac{1}{4}{\Delta_x}^2 B(\rho_L-\rho_V)$ and the lower slab with volume $\frac{1}{2}\Delta_x B$ and gravitational energy $-\frac{1}{4}{\Delta_x}^2 B(\rho_S-\rho_L)$. Taking into account the definition of G, we add a term:

$$\mathcal{F}_g=\Delta_x G\left(\sum_{x=U_L}^{U_R}H_x^2-\Delta_\rho\sum_{x=D_L}^{D_R}h_x^2-(1-\Delta_\rho)\Delta_x B\right) \quad ,$$

which indeed has no contribution for $\Delta_\rho=0$. Dividing by $\gamma_{LV}\Delta_x$ to make it dimensionless:

$$f_g=\frac{\Delta_x G}{\gamma_{LV}\Delta_x}\left(\sum_{x=U_L}^{U_R}H_x^2-\Delta_\rho\sum_{x=D_L}^{D_R}h_x^2-(1-\Delta_\rho)\Delta_x B\right)$$

The relevant parameters for the gravitational energy are now the dimensionless numbers G/γ_{LV} and Δ_ρ.

5.5 An attempt at including the elastic energy

Here we will make an attempt at finding an appropriate way to include the elastic energy. Discretizing this term is far less straightforward than the others. We have made a number of approximations and workarounds to get it working numerically. As such, this treatment is far from elegant and it leaves much room for improvement. However, as we will see in section 6, the results we obtain with this method are not bad.

Starting from the expression in 4.3:

$$\mathcal{F}_E=\frac{E}{4\pi}\int_{-\infty}^{\infty}\frac{2|q|}{3}\hat{h}(q)\hat{h}(-q)dq \quad ,$$

we first have to define the discrete Fourier transform of $h(x)$. Because h(x) is only nonzero on the domain $[-R,+R]$, we have that:

$$\hat{h}(q)=\int_{-\infty}^{\infty}h(x)e^{iqx}dx=\int_{-R}^{+R}h(x)e^{iqx}dx \tag{4}$$

We replace the integral by a sum over all h_x (picking up a factor of Δ_x to get the correct dimensionality), split into a real and an imaginary part, and make sure that x is defined so that $x = 0$ is at the middle of the droplet. Keep in mind that q has dimensions 1/distance:

$$\hat{h}_q = \frac{\Delta_x^2}{2} \sum_{x=0}^{D_R - D_L} h_{x+D_L} \left(\cos\left[q\Delta_x \left(x - \frac{D_R - D_L}{2} \right) \right] + i \sin\left[q\Delta_x \left(x - \frac{D_R - D_L}{2} \right) \right] \right)$$

Given that $\cos(-q) = \cos(q)$ and $\sin(-q) = -\sin(q)$, we also know the discrete version of $\hat{h}(-q)$:

$$\hat{h}_{-q} = \frac{\Delta_x^2}{2} \sum_{x=0}^{D_R - D_L} h_{x+D_L} \left(\cos\left[q\Delta_x \left(x - \frac{D_R - D_L}{2} \right) \right] - i \sin\left[q\Delta_x \left(x - \frac{D_R - D_L}{2} \right) \right] \right)$$

We now need to discretize the integral over Fourier space. We do not have any immediate reason to assume that this integral converges. That is problematic. To solve this issue, we look to the definition of what this space actually represents. An integral over q-space must be over all possible values of q; i.e. over all possible wavenumbers involved in the integral. But here we can already see that in our discrete approximation, there must be a maximum wavenumber. Because we have discretized h_x, we only have information about the points of the surface corresponding to the set of depths h_x. These points have a horizontal separation of Δ_x. We therefore define a maximum wavelength $q_{max} = 2\pi/\Delta_x$, which is the lowest wavenumber of which have no information about its occurance in the system.

If we were to construct $h(x)$ from displacements of the form $\epsilon \cos qx$, then as we approach q_{max}, we are effectively describing smaller and smaller differences in height. Given the fact that our discretized approach is an approximation, the accuracy of describing smaller and smaller length scales becomes worse and worse. To illustrate, consider the bottom row of figure 7. There is a large peak around q_{max}, which contributes significantly to the elastic energy even though it is the result of very small differences in height (see also figure 6). Taking into account the contributions of these wavenumbers would effectively decrease the accuracy of our simulation. Thus, we will neglect their contributions, and only look at lower wavenumbers. We truncate the integral over q-space at the minimum of the envelope of $h(q)$, giving the domain $[0, \pi/\Delta_x]$. We also simplify the integral by using the following: given that we can split $\hat{h}_q$ and $\hat{h}_{-q}$ into a real and an imaginary part, their product will be of the form of $(a + ib)(a - ib) = a^2 + b^2$. Going from an intergral to a sum over q gives us an extra unit of $1/\Delta_x$ to get the appropriate dimensionality. We then obtain:

$$\mathcal{F}_E = \frac{E\Delta_x^3}{16\pi} \sum_{q=0}^{\pi/\Delta_x} \frac{2|q|}{3} \left(\left(\sum_{x=0}^{D_R - D_L} h_{x+D_L} \cos\left[q\Delta_x \left(x - \frac{D_R - D_L}{2} \right) \right] \right)^2 + \left(\sum_{x=0}^{D_R - D_L} h_{x+D_L} \sin\left[q\Delta_x \left(x - \frac{D_R - D_L}{2} \right) \right] \right)^2 \right)$$

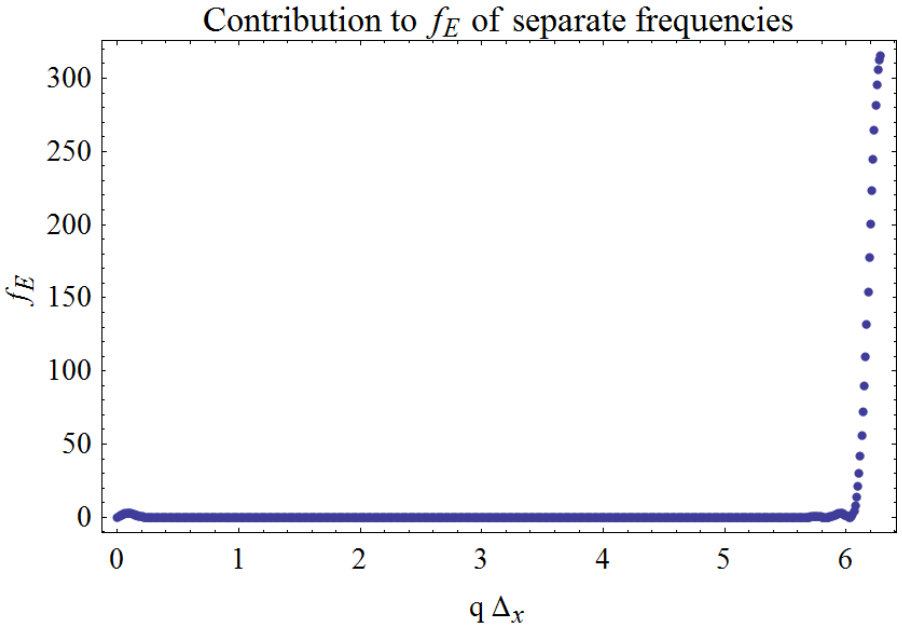

Figure 6: A second peak around q_{max}. While its presence is very uncertain, its contribution dominates that of the lower wavenumbers.

As long as the integral does not diverge within the domain $[0, \pi/\Delta_x]$, the elastic energy will be finite. Given that the droplet has a finite size and that $h(x)$ is therefore only defined on a finite domain, we suspect that it will not diverge for $q \to 0$. Displacements with $q \to 0$ would be nearly flat displacements of the entire interface. Pure translations of the interface do not have any contributions to the elastic energy, so we expect that for $q \to 0$, the integrand must go to zero. As seen in the top right image of figure 7, this is indeed what happens.

There are two more things we need to address. The first is that we need to specify the number of points in Fourier space (N_q) we want to use. Given that the expression is order $\mathcal{O}(N_q * (D_R - D_L))$ and that we need to calculate it for M Metropolis cycles, we want to keep this to a minimum. On the other hand, the resolution in q-space must be high enough to adequately describe the function. For this we have to take a look at the functions $\hat{h}(q)$ for typical droplet shapes. From trial and error we found that for our parameters $N_q = 60$ had a good balance.

The last detail we need to address to finalize our numerics on the elastic energy is this: by using equation 4 we have neglected the part of the interface that is spanned between h_{D_L}, h_{D_R} and the base of the droplet B. To take this into account, we add two points, in the middle between the base and the outermost points. The leftmost point has coordinates $\{x_L, z_L\} = \{-B + \frac{B-(D_R-D_L)}{2}, \frac{h_{D_L}}{2}\}$ and the rightmost has coordinates $\{x_R, z_R\} = \{+B - \frac{B-(D_R-D_L)}{2}, \frac{h_{D_R}}{2}\}$. We add these to h_q so that the terms we referred to as 'a' and 'b' become:

$$a = z_L \cos\left[q\Delta_x\left(x_L - \frac{D_R - D_L}{2}\right)\right] + z_R \cos\left[q\Delta_x\left(x_R - \frac{D_R - D_L}{2}\right)\right] + \sum_{x=0}^{D_R-D_L} h_{x+D_L} \cos\left[q\Delta_x\left(x - \frac{D_R - D_L}{2}\right)\right]$$

$$b = z_L \sin\left[q\Delta_x\left(x_L - \frac{D_R - D_L}{2}\right)\right] + z_R \sin\left[q\Delta_x\left(x_R - \frac{D_R - D_L}{2}\right)\right] + \sum_{x=0}^{D_R-D_L} h_{x+D_L} \sin\left[q\Delta_x\left(x - \frac{D_R - D_L}{2}\right)\right]$$

Dividing the entire expression by $\gamma_{LV}\Delta_x$ gives us the dimensionless expression we will use, with a and b as above:

$$f_E = \frac{E\Delta_x^2}{16\pi\gamma_{LV}} \sum_{q=0}^{\pi/\Delta_x} \frac{2|q|}{3}\left(a^2 + b^2\right) \tag{5}$$

The relevant parameter for the scale of the elastic energy is now the dimensionless number $E\Delta_x^2/\gamma_{LV}$. This concludes our discussion on the numerics of the elastic energy.

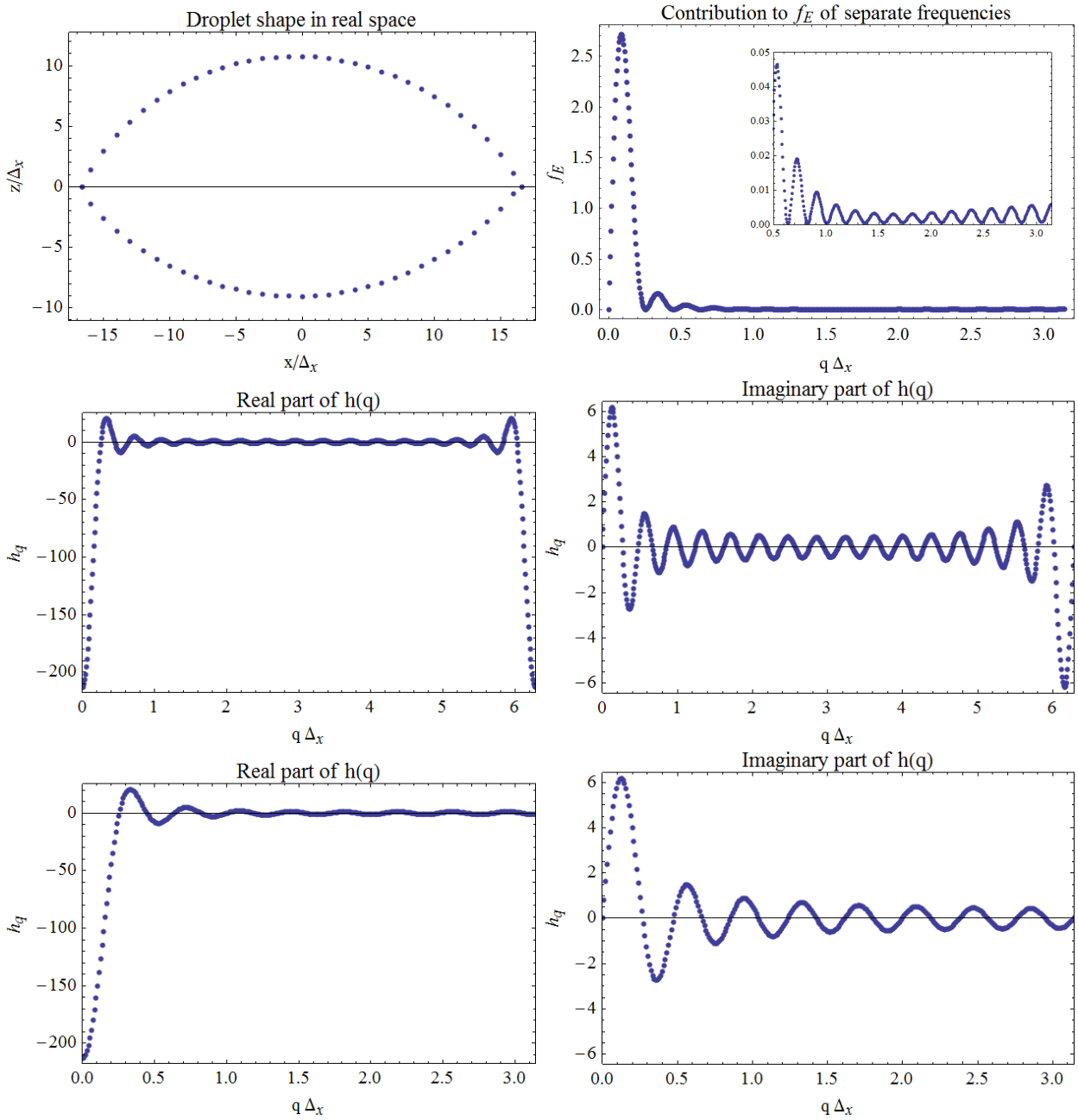

Figure 7: **Top left:** droplet shape in real space. (Parameters used: $G/\gamma_{LV} = 0$, $E\Delta_x^2/\gamma_{LV} = 10^{-5}$, $\gamma_{SV}/\gamma_{LV} = 1$, $\gamma_{SL}/\gamma_{LV} = 1$, $M = 2 * 10^3$, $T_{in} = 0.2$). **Top right**: the integrand $\hat{Q}(q)\hat{h}(q)\hat{h}(-q)$ in q-space and zoomed in. **Middle row:** the real and imaginary parts of $\hat{h}(q)$ in q-space on the domain $[0, 2\pi/\Delta_x]$. **Bottom row:** the real and imaginary parts of $\hat{h}(q)$ in q-space on the domain $[0, \pi/\Delta_x]$. The sum over entire q-space (equation 5) does not converge.

6 Results

6.1 Comparison with Soligno's results: rigid solid

The case studied by Soligno [6] can be replicated within our simulation by taking the limit of $E\Delta_x^2/\gamma_{LV} \to \infty$ In this case, it should matter little what the precise expression for the elastic energy is, as the cost of having volume in the lower array will be so high that it will be completely depleted. Soligno also provided analytical expressions determining the shape of a droplet with a certain volume and contact angle in the case of a perfectly rigid solid. We can determine the contact angle directly from our chosen parameter values. Rewriting Young's law in terms of our parameters γ_{SL}/γ_{LV} and γ_{SV}/γ_{LV}:

$$\gamma_{SV} - \gamma_{SL} = \gamma_{LV}\cos\theta \to \cos\theta = \frac{\gamma_{SV}}{\gamma_{LV}} - \frac{\gamma_{SL}}{\gamma_{LV}}$$

The analytical expression we compare our numerical solution with is the solution for $z(x)$ of the following equation [6]:

$$x^2 + z(x)^2 + 2z(x)\left(\frac{V}{\theta - \cos\theta\sin\theta}\right)^{1/2}\cos\theta - \frac{V\sin^2\theta}{\theta - \cos\theta\sin\theta} = 0$$

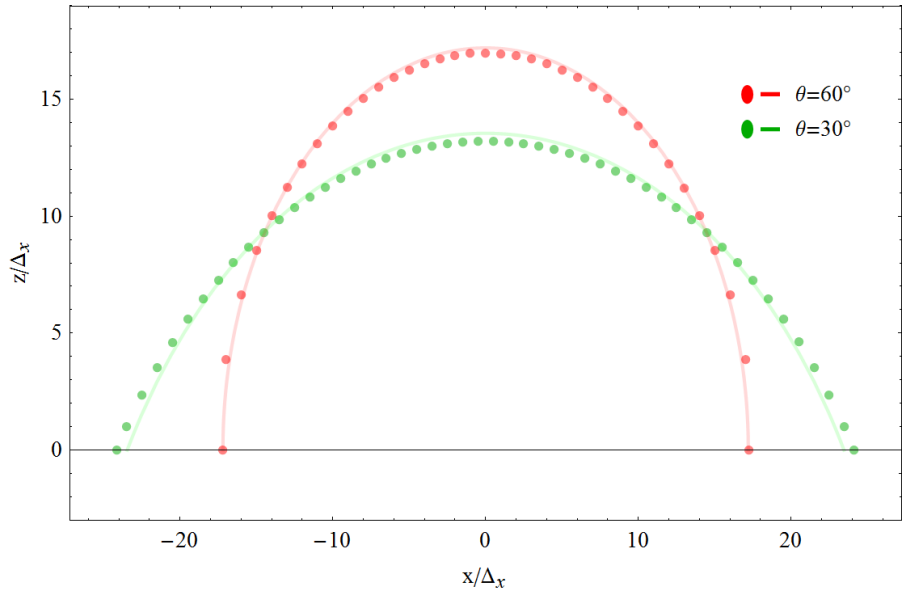

Figure 8: The dots indicate our numerical results. The linse give the analytical solution provided by Soligno. For these results we have used $\gamma_{SL}/\gamma_{LV} = 1$, $\gamma_{SV}/\gamma_{LV} = 1$ (red), $\gamma_{SV}/\gamma_{LV} = 1.5$ (green). We have $V = 500\Delta_x^2$, $T_{init} = 0.2$ and $M = 10^5$. The elasticity is given by $E\Delta_x^2/\gamma_{LV} = 0.1$, causing the lower array to be completely depleted. For all intents and purposes, this mimics the infinitely rigid limit.

As we can see from figure 8, the agreement is reasonable. Our simulation generates roughly the same shape and contact angles as the analytical solution. The agreement is, however, not perfect. This could be a result of choosing M too low, which results in a lower quality of the solution. It could also be a systematic error in our code, but we would have to dig deep to find the cause. The agreement is good enough for qualitative analysis of the results, so we will explore it no further.

6.2 Surface terms only

Before we try to add elasticity to our system, let's observe what happens when we change the ratios of the surface energies. These results will mimic a droplet in a fluid-fluid interface. We will continue to use the subscript S to denote the "bottom" phase for convenience.

6.2.1 Varying γ_{SV} with respect to γ_{LV} and γ_{SL}

As we can see in figure 9, increasing $\gamma/\gamma_{SV} = \gamma_{LV}/\gamma_{SV} = \gamma_{SL}/\gamma_{SV}$ causes the droplet shape to become more and more circular. This behaviour can also be deduced quite simply from the expression for the surface energy.

$$f_S = \frac{\gamma_{LV}}{\gamma_{SV}}A_{LV} + \frac{\gamma_{SL}}{\gamma_{SV}}A_{SL} - B$$

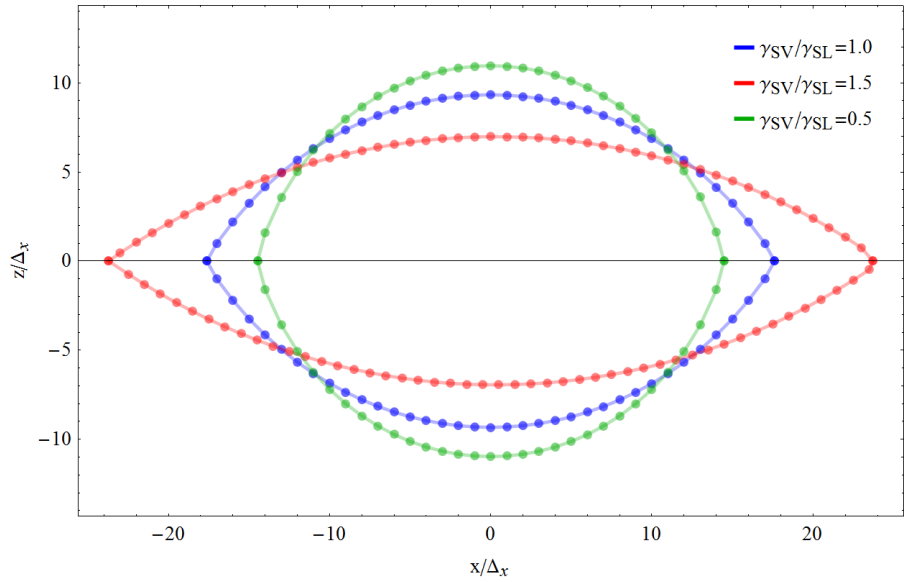

Figure 9: For these results we have used $\gamma_{SL}/\gamma_{LV} = 1$, $V = 500\Delta_x^2$, $T_{init} = 0.2$ and $M = 10^6$. The only contributions to the free energy are the surface terms. Gravity and elasticity are not included i.e. $G/\gamma_{LV} = 0$ and $E\Delta_x^2/\gamma_{LV} = 0$.

If the ratios of the γ's increase, their contribution relative to that of the base will become larger. Minimizing the fluid-liquid interfacial areas will become more important than widening the base. As we know, the shape with the lowest surface/volume ratio is a circle for two dimensions, and a sphere for three.

6.2.2 Varying γ_{SL} with respect to γ_{LV}

We can also change only one of the ratios. We here show the results for changing the surface free energy of the SL interface. This will cause it to become energetically more expensive than the LV interface. We could expect, then, that the interface on the more expensive side will become smaller and smaller for increasing γ_{SL}/γ_{LV}.

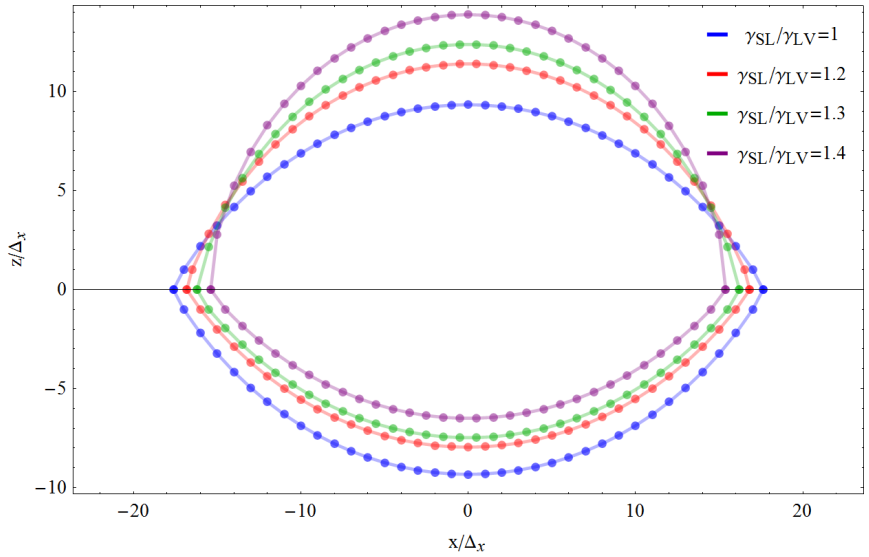

Figure 10: For these results we have used $V = 500\Delta_x^2$, $T_{init} = 0.2$, $\gamma_{SV}/\gamma_{LV} = 1$, $E\Delta_x^2/\gamma_{LV} = 0$, $G/\gamma_{LV} = 0$ and $M = 5 * 10^5$.

Figure 10 indeed shows the SL interface shrinking, and the LV interface increasing in size. There is also a small decrease in width which we had not predicted.

6.3 Gravity

For the sake of completeness, let us also take a look at the effects of gravity. We would expect a net volume shift from the upper to the lower array for $\Delta_\rho = 1$, which is the case for a droplet suspended in a fluid-fluid interface where both fluids have the same density. We would not expect much else to happen, except perhaps a small decrease in width as in figure 10. So let's take a look:

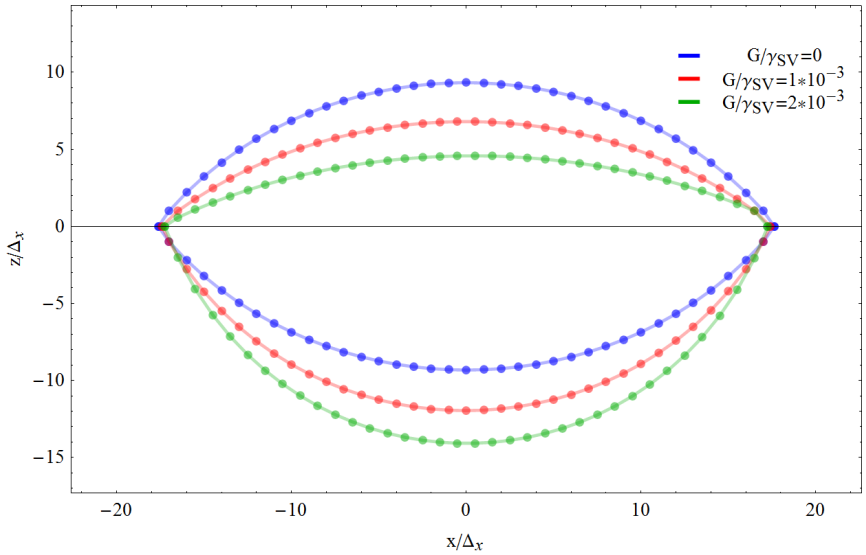

Figure 11: For these results we have used $V = 500\Delta_x^2$, $T_{init} = 0.2$, $\gamma_{LV}/\gamma_{LV} = 1$, $\gamma_{SL}/\gamma_{LV} = 1$, $E\Delta_x^2/\gamma_{LV} = 0$, $\Delta_\rho = 1$ and $M = 5 * 10^5$.

As we can see from figure 11, there is indeed a net volume shift to the lower part of the droplet. There also appears to be a *tiny* decrease in width. Basically, gravity works the way we expect it to.

6.4 Results with elasticity, rigid and soft limits

And now we arrive at the most interesting part of the thesis. We've done a lot of work on including this elasticity of the solid, but does it actually work? Well, first we have to look at what we expect would happen. For this, we want to look at what happens for very rigid and very soft solids. A useful back-of-the-envelope type of derivation to observe the behaviour of different limits of the elastic modulus can be done by considering a simple one-dimensional spring. Its energy is given by:

$$U = \frac{1}{2}Cx^2$$

The force exerted by this spring to try and push or pull it back to its equilibrium position is:

$$F = Cx$$

For a equilibrium configuration, this force must balance out the capillary force exerted by the liquid droplet on the solid surface. Assuming this capillary force is constant and independent of the elastic modulus, the force F must also be constant. This allows us to rewrite the elastic energy in an equilibrium configuration in terms of constants:

$$x = F/C \qquad\qquad U = \frac{1}{2}C\left(\frac{F}{C}\right)^2 = \frac{1}{2}\frac{F^2}{C}$$

In the limits of perfectly rigid solids ($C \to \infty$) we can see that both the displacement and the elastic energy will go to zero. In this limit we can also neglect the free energy cost of additional surface with respect to the elastic contribution to the free energy. This indicates that for a perfectly rigid solid, we indeed retrieve the limit where all liquid will rest on top of the solid, and no solid will be displaced. In this limit we retrieve the case where Young's law holds. The other limit, of infinitely soft solids ($C \to 0$), can also be scouted this way. For a given displacement x, we can now safely neglect the elastic contribution, and state that the droplet shape will be dominated by surface terms. This will lead to the case of a liquid lens. If we assume that the elastic modulus C of our shamefully simple derivation is at least proportional to the elastic modulus E in our expression for the elastic energy, we can apply these above predictions to our two-dimensional system and see if they match.

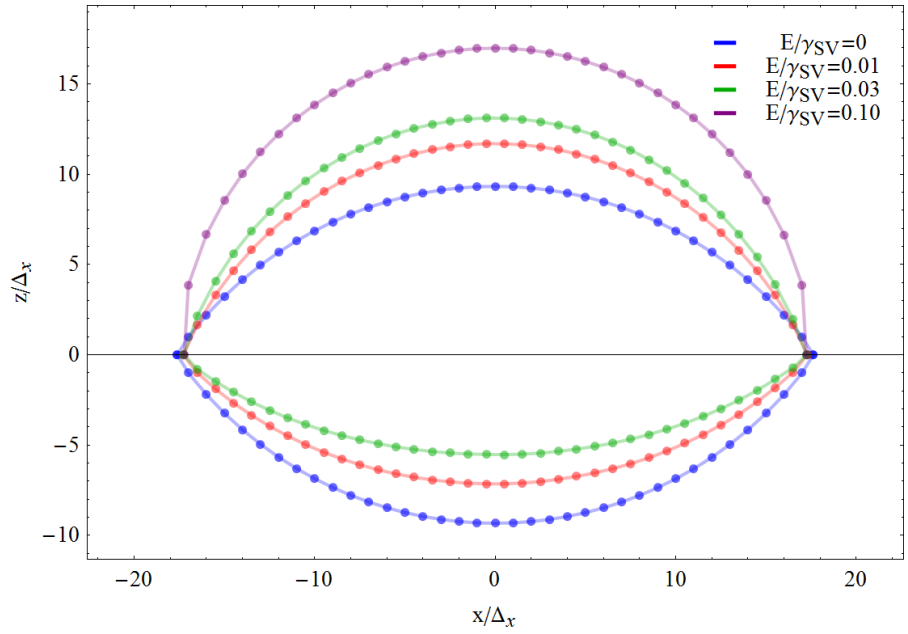

Figure 12: Droplet shapes for different values of E/γ_{SV}. Other parameters used are $V = 500\Delta_x^2$, $G/\gamma_{LV} = 0$, $\gamma_{SL}/\gamma_{LV} = 1$, $\gamma_{SV}/\gamma_{LV} = 1$, $T_{in} = 0.2$ and $M = 2 * 10^4$. For $E/\gamma_{SV} = 0.10$ the lower array is completely depleted.

From figure 12 we can see that we retrieve the infinitely soft limit of a liquid lens and the infinitely rigid limit of a hard floor. The contact angle θ we retrieve here should be 90 degrees, in accordance with $\gamma_{SL}/\gamma_{LV} = 1$ and $\gamma_{SV}/\gamma_{LV} = 1$. From the figure, we see that this is indeed the case. We can also simulate values in between the two limits with our simulation, as is evident from the red and green lines. From these results, I conclude that I've accomplished what I set out to do: to write a code that can calculate the shape of a droplet for a large range of physical parameters, taking into account the effects of interfacial energy costs, gravity and most importantly elasticity. The way I've included elasticity might not be the best or the most elegant way, but it is *a* way.

7 Appendix: on pendant droplets

This last section is dedicated to anyone who would try to replicate my work. It pertains to the possibilities but more importantly the limitations of the method described in this thesis. The most notable limitation of this method is that it is impossible to calculate the shape of pendant droplets. Due to the fact that we require a uniquely valued $h(x)$, we are limited to contact values of $\theta \leq 90°$. However, it is possible to adjust the method in such a way that higher contact angles can be simulated. The only component that requires $h(x)$ to be single-valued for every x is the elastic component, one could describe the other part of the droplet by horizontal (wide) slabs instead of vertical (tall) rectangles, as done by Soligno [6]. This hybrid scheme should in theory be able to simulate pendant droplets as well as sessile ones. In such a hybrid scheme, one has to however take care in the swaps that are allowed. I have personally tried to create this scheme, but ran into problems I suspect spring from the principle of detailed balance[5]. To equilibrate a system where the two arrays are inherently of different sizes, one needs to take a careful look at the probabilities of each swap. I have chosen to forgo this hassle, and restrict myself to small contact angles.

[5]The principle of detailed balance is succinctly described as following: *at equilibrium, each elementary process should be equilibrated by its reverse process.*

References

[1] L.A. Lubbers, J.H. Weijs, L. Botto, S. Das, B. Andreotti, J.H. Snoeijer, *Drops on soft solids, Free energy and double transition of contact angles, Journal of Fluid Mechanics*, 747, R1 doi:10.1017/jfm.2014.152

[2] Didier Long, Armand Ajdari, Ludwik Leibler, *Static and Dynamic Wetting Properties of Thin Rubber Films*, *ACS:Langmuir*, 1996, 12 , 5221-5230

[3] Glenn H. Frederickson, Armand Ajdari, Lubwik Leibler, Jean-Pierre Carton, *Surface Modes and Deformation Energy of a Molten Polymer Brush*, *ACS:Macromolecules*, 1992, 25, 2992-2889

[4] Joost H. Weijs, Bruno Andreotti, Jacco H. Snoeijer, *Elasto-Capillarity at the nanoscale: on the coupling between elasticity and surface energy in soft solids*, *Soft Matter*, 2013, 9, 8494

[5] Joost H. Weijs, Bruno Andreotti, Jacco H. Snoeijer, *Capillarity of soft amorphous solids: a microscopic model for surface stress*, *Phys. Rev.* E 89, 042408

[6] Giuseppe Soligno, *Progress report*

[7] Das, S., Marchand, A., Andreotti, B., Snoeijer, J. H.: *Elastic deformation due to tangential capillary forces* Phys. Fluids 23 (7), 2011, 072006.

[8] Robert. W. Style, Eric. R. Dufresne: *Static wetting on deformable substrates, from liquids to soft solids* Soft Matter, 2012,8, 7177-7184

[9] R. Shuttleworth, *The surface tension of solids*, Proc. Phys. Soc., London Sect. A 63, 444 (1950).